

# Asymptotic behavior of the electron cloud instability

Samuel A. Heifets

*Stanford Linear Accelerator Center, Stanford University, Stanford, CA 94309, USA\**

## Abstract

The fast beam-ion instability and the single bunch electron-cloud instability are substantially nonlinear phenomena and can be analyzed in a similar way. The initial exponential growth of the amplitudes known for both instabilities takes place only in the linear approximation. Later, in the nonlinear regime, amplitudes grow according to a power law or even decrease. We analyze the nonlinear regime describing the growth of amplitudes in time and along the train of bunches. Analytic analysis is compared with simulations.

PACS numbers: 29.27.Bd, 29-20-Dh, 41-60, 52-59-f

## 1 Introduction

The electron cloud instability [1],[2] and the fast ion instability (FII) are driven by the interaction of a beam with the cloud of surrounding particles. Analysis of the instabilities were mostly carried out in the linear approximation [2],[3]. That is quite sufficient for determining the thresholds and for evaluating methods to mitigate instabilities. However, the growth time of the linear approximation is usually very small, in the best cases of the order of 100 – 200  $\mu s$ , making difficult direct observation of the linear stage of instability. Actually, the exponential growth of the linear approximation is restricted to the time interval of the order of the growth time and is quickly replaced by a slow growth. It is clear that the motion of particles in the latter regime is substantially nonlinear. This is especially true for the particles of the cloud. It is important to study the nonlinear regime because only this regime may be observed in experiments and because the study can predict the level at which the instabilities saturate clarifying mechanisms of their stabilization. Another motivation is search of a method to speed up numeric solutions of the equations of motion which at the present time are very time consuming. The earlier attempts to address the effect of nonlinearity were carried out [4] even somewhat earlier than the wake field of the electron cloud was determined in the linear approximation [3]. Such analysis allowed to find, in particular, the  $Q$ -factor of the wake. However, the method

*Presented at ELOUD07, 4/9/2007-4/12/2007, Daegu, South Korea*

used at that time was very cumbersome. The saturation of the instability observed in simulations was also predicted [5], [6], but the papers had mostly qualitative character.

In this paper, we study the instabilities emphasizing the nonlinear character of the motion. We consider mostly the single bunch electron cloud instability assuming that the cloud remains the same on each turn. Results obtained for electron cloud are easily modified for the FII. In the analysis we consider a simple 1D model, however, results can be easily generalized for more realistic Bassetti-Erskine interaction [7].

In the next section we introduce notations and, for the sake of completeness, reproduce the well known result of the linear. In section 3 we consider the quasi-linear regime. Consideration is based on the single mode approximation considered. In particular, we obtain parameters of the electron cloud wake including the  $Q$ -factor and show results of direct numeric solution of the equation of motion. To proceed further, we obtain simplified equation for the amplitude of oscillations applicable to the nonlinear regime using averaging method. That allows us to refine analysis of the linear regime, consider correction to the exponential regime due to nonlinearity of motion, and predict power law for the transition from exponential to nonlinear regimes. In the last section, we solve nonlinear equations for the amplitudes numerically and compare results with the previous analysis. In conclusion, we discuss applicability of the approach to the fast ion instability and summarized results.

## 2 Basic equations of motion

Let us consider a relativistic particle interacting with the cloud of electrons or ions. We describe a bunch as a set of macro-particles each representing a slice of the bunch and distributed longitudinally with the rms  $\sigma_z$ . The transverse offset of a macro-particle is  $\tilde{y}_c(s, z)$ , where  $z > 0$  is the distance of a slice from the head of the bunch. Location of the slice  $z$  around the ring at the moment  $t$  is  $s = ct - z$ . The offset of a particle of the cloud is denoted by  $\tilde{Y}(s, t)$  at the moment  $t$ . We use the usual notations for bunch population  $N_B$ , transverse rms dimensions of the bunch  $\sigma_{x,y}$ , and the classical radius of electron  $r_e$ .

In the ultra-relativistic case, the interaction can be described as a kick integrating Coulomb force over the very short time of interaction (neglecting the shift of particles during the interaction). Equation of motion for a cloud particle take the form

$$\begin{aligned} & \frac{\partial^2 \tilde{y}_c(s, z)}{\partial s^2} + \left(\frac{\omega_y}{c}\right)^2 \tilde{y}_c(s, z) \\ &= \frac{2r_e \lambda_c}{\gamma} \frac{\tilde{Y}(s, \frac{s+z}{c}) - \tilde{y}_c(s, z)}{\sigma_y(\sigma_x + \sigma_y)} G_y \left[ \tilde{Y}(s, \frac{s+z}{c}) - \tilde{y}_c(s, z), \tilde{X}(s, \frac{s+z}{c}) - \tilde{x}_c(s, z) \right], \quad (1) \end{aligned}$$

$$\begin{aligned} & \frac{\partial^2 \tilde{Y}(s, t)}{\partial t^2} \\ &= -\Omega_y^2 [\tilde{Y}(s, t) - \tilde{y}_c(s, ct - s)] G_y [\tilde{Y}(s, t) - \tilde{y}_c(s, ct - s), \tilde{X}(s, t) - \tilde{x}_c(s, ct - z)], \end{aligned} \quad (2)$$

where  $\omega_y$  and  $\Omega_y$ ,

$$\left(\frac{\Omega_y}{c}\right)^2 = \frac{2\lambda_b r_e}{\sigma_y(\sigma_x + \sigma_y)}, \quad (3)$$

are the angular frequency of small amplitude oscillations of the beam and cloud particles, respectively,  $\lambda_b = N_B/\sqrt{2\pi\sigma_z^2}$  and  $\lambda_c$  are the linear density of the bunch and cloud, respectively.

The function  $G_y(x, y)$  is given by the well known Bassetti-Erskine formula normalized by  $G_y(0, 0) = G_x(0, 0) = 1$ . In the asymptotic  $\xi, \eta \gg \sigma_{x,y}$ ,

$$G_y(\xi, \eta) \rightarrow \frac{\sigma_y(\sigma_x + \sigma_y)}{\xi^2 + \eta^2}. \quad (4)$$

It is tempting to assume that the cloud can also be described as a set of rigid slices with the rms dimensions  $\sigma_{c,x}, \sigma_{c,y}$  with the coordinates of the centers oscillating as  $X_c(s, t)$ , and  $Y_c(s, t)$ . Averaging equation of motion with such distribution would reduce the problem of beam-cloud interaction to much simple problem of motion of centers of slices. Equation of motion depend in this case only on  $\Sigma_{x,y}$ ,  $\Sigma_{x,y}^2 = \sigma_{x,y}^2 + \sigma_{c,(x,y)}^2$ , and can be linearized if  $|X_c - x_c| \ll \Sigma_x$ ,  $|Y_c - y_c| \ll \Sigma_y$ . That would mean that the amplitudes of bunch oscillations grow exponentially in the linear regime at least until it becomes comparable with the rms of the cloud. This, however, contradicts to all existing simulations. Therefore, representation of the cloud as a set of rigid slices is invalid. For our analysis, we use, therefore, Eqs. (1), (2) reducing the bunch but not the cloud to a set of rigid macroparticles. We believe that is justified because the rms of the bunch is much smaller than the rms of the cloud.

It is convenient to use dimensionless coordinates  $\tau = \omega_y s/c$  instead of  $s$  and  $\zeta = \Omega_y z/c$  instead of  $z$ . We define and use below functions  $y_c(\tau, \zeta)$  and  $Y(\tau, \zeta)$  related to the offsets in units of  $\sigma_y$ ,

$$y_c(\tau, \zeta) = \tilde{y}_c\left(\frac{c\tau}{\omega_y}, \frac{c\zeta}{\Omega_y}\right)/\sigma_y, \quad Y(\tau, \zeta) = \tilde{Y}\left(\frac{c\tau}{\omega_y}, \frac{\tau}{\omega_y} + \frac{\zeta}{\Omega_y}\right)/\sigma_y. \quad (5)$$

Equations of motion in these variables take the form

$$\begin{aligned} & \frac{\partial^2 y_c(\tau, \zeta)}{\partial \tau^2} + y_c(\tau, \zeta) = \Lambda \{ [Y(\tau, \zeta) - y_c(\tau, \zeta)] G_y [Y(\tau, \zeta) - y_c(\tau, \zeta), X(\tau, \zeta) - x_c(\tau, \zeta)] \}, \\ & \frac{\partial^2 Y(\tau, \zeta)}{\partial \zeta^2} = - [Y(\tau, \zeta) - y_c(\tau, \zeta)] G_y [Y(\tau, \zeta) - y_c(\tau, \zeta), X(\tau, \zeta) - x_c(\tau, \zeta)], \end{aligned} \quad (6)$$

where

$$\Lambda = \frac{2r_e}{\gamma} \frac{\lambda_c}{\sigma_y(\sigma_x + \sigma_y)} \left(\frac{c}{\omega_y}\right)^2. \quad (7)$$

The angular brackets in the first equation mean averaging with the distribution function over initial conditions for the cloud particles.

Although equations for the bunch and the cloud are written in terms of  $\tau$  and  $\zeta$ , we have to remember that the meaning of these variables in two cases is different. While  $\tau$  plays the role of time for the bunch and  $\zeta$  numbers bunch slices, for the cloud  $\zeta$  plays the role of time and  $\tau$  defines position of the particle in the ring. Respectively, for the bunch  $\tau$  goes from zero to infinity while, for the cloud,  $\tau$  is limited by one turn provided the cloud is regenerated on each turn.

The growth rate in the linear approximation for the horizontal plane is obtained replacing  $\Lambda$  by  $(\sigma_y/\sigma_x)^2 \Lambda$ . For a flat beam,  $\sigma_y \ll \sigma_x$ , the growth rate is much slower than in the vertical plane. That allows us to reduce the problem to 1D problem replacing  $G_y(X, Y)$  by  $G(Y)$ .

In the following, to simplify calculations, we may replace  $G(Y)$  by

$$G(Y) = \frac{1}{1 + \kappa_0^2 Y^2}, \quad \kappa_0^2 = \frac{1}{\sigma_x \sigma_y}, \quad (8)$$

which behaves in the same way at small and large  $Y$  as exact function  $G$ .

1D equations takes the form

$$\frac{\partial^2 y_c(\tau, \zeta)}{\partial \tau^2} + y_c(\tau, \zeta) = \Lambda \langle [Y(\tau, \zeta) - y_c(\tau, \zeta)] G[Y(\tau, \zeta) - y_c(\tau, \zeta)] \rangle, \quad (9)$$

$$\frac{\partial^2 Y(\tau, \zeta)}{\partial \zeta^2} = -[Y(\tau, \zeta) - y_c(\tau, \zeta)] G[Y(\tau, \zeta) - y_c(\tau, \zeta)]. \quad (10)$$

We assume the initial conditions  $Y(\tau, 0) = Y_0$ ,  $(\partial Y(\tau, \zeta)/\partial \zeta)_{\zeta=0} = 0$  corresponding to cloud particles at rest at the moment  $\zeta = 0$  (i.e. at  $t_0 = s/c$  when the head of a bunch arrives at the location  $s$ .)

The form of  $G(Y - y_c)$  can be simplified further re-scaling variables and write  $G$  in the form

$$G(Y) = (1 + Y^2)^{-1}. \quad (11)$$

## 2.1 Linear regime

For small amplitudes, Eqs. (9)-(10) can be linearized replacing  $G_{x,y} \rightarrow 1$ . Equations for horizontal and vertical motion in this approximation are independent. For  $y$ -motion, the averaging over the cloud distribution gives:

$$\begin{aligned}\frac{\partial^2 y_c(\tau, \zeta)}{\partial \tau^2} + y_c(\tau, \zeta) &= \Lambda[\langle Y(\tau, \zeta) \rangle - y_c(\tau, \zeta)], \\ \frac{\partial^2 \langle Y(\tau, \zeta) \rangle}{\partial \zeta^2} &= -[\langle Y(\tau, \zeta) \rangle - y_c(\tau, \zeta)].\end{aligned}\quad (12)$$

Eqs. (12) lead to the beam instability [2]. Solution for the slice can be found in the form

$$y_c(\tau, \zeta) = a(\tau, \zeta) \sin(\tau\sqrt{1 + \Lambda} - \zeta), \quad (13)$$

where  $a$  is a slow function of the arguments. The second of Eq. (12) shows that  $\langle Y(\tau, \zeta) \rangle$  has the similar form but with the phase shift,

$$\langle Y(\tau, \zeta) \rangle = A(\tau, \zeta) \cos(\tau\sqrt{1 + \Lambda} - \zeta), \quad (14)$$

where, again,  $A$  is a slow function of the arguments. Here we retain only induced oscillations neglecting the free oscillations. The latter depend on the initial conditions for the cloud and does not contribute to instability.

Eqs. (12) can be written as equations for the amplitudes  $a$ ,  $A$ . Neglecting small terms of the order of  $(\partial a/\partial \tau)^2$ ,  $(\partial^2 a/\partial \tau^2)$ ,  $(\partial A/\partial \zeta)^2$ ,  $(\partial^2 A/\partial \zeta^2)$  and averaging over the fast oscillations it is easy to get for  $\Lambda \ll 1$ ,

$$\frac{\partial a}{\partial \tau} = \frac{i\Lambda}{2} \langle A(\tau, \zeta) \rangle, \quad \frac{\partial A}{\partial \zeta} = -\frac{i}{2} a(\tau, \zeta). \quad (15)$$

Two equations can be combined into

$$\frac{\partial^2 a(\tau, \zeta)}{\partial \tau \partial \zeta} = \frac{\Lambda}{4} a(\tau, \zeta), \quad (16)$$

which can be reduced to the ordinary differential equation for  $a(x)$  using variable  $x = \tau\zeta$ ,

$$\frac{d}{dx} \left( x \frac{d}{dx} a(x) \right) = \frac{\Lambda}{4} a(x). \quad (17)$$

Exact solution of Eq. (17) is given in terms of the Bessel function with the initial condition  $a(\tau, 0) = a_0$ ,

$$a(x) = a_0 I_0(\sqrt{\Lambda x}). \quad (18)$$

For large  $\Lambda x \gg 1$ , Eq. (18) gives the well known result [2], citeGS

$$a(\tau, \zeta) = \frac{a_0}{\sqrt{2\pi}} \frac{1}{(\Lambda\tau\zeta)^{1/4}} e^{\sqrt{\Lambda\tau\zeta}}. \quad (19)$$

Note that result is independent of the initial condition for the cloud.

The amplitude  $A(s, t)$  of induced oscillations of a particle in the cloud grows in time as

$$A(\tau, \zeta) = \frac{\zeta}{\sqrt{\Lambda\tau\zeta}} a(\tau, \zeta). \quad (20)$$

Parameter  $\Lambda\tau\zeta \simeq 1$  in the linear regime. Therefore, the ratio of amplitudes  $A/a$  depends mostly on parameter  $\zeta = \Omega_b z/c$ . The ratio is of the order of one for the e-cloud. For ions the ratio can be large meaning that the ion density is defined by the instability itself.

### 3 Quasi-linear regime

For  $y_c = 0$  (the beam is fixed), Eq. (10) describes 1D nonlinear oscillator. At small amplitudes, a particle oscillates along the beam line with the frequency  $\nu = 1$ . At larger amplitudes, the frequency of oscillations  $\nu(Y_0)$  depends on the amplitude  $Y_0$  and there are harmonics of motion  $e^{ik\nu\zeta}$ ,  $k = 1, 2, \dots$ , with frequencies multiple of  $\nu(Y_0)$ . Generally, each harmonics modulates the bunch leading to the e-cloud instability. For some parameters, the growth rate caused by each mode may become comparable with the mode separation  $\simeq \nu(Y_0)$ . In this case, the harmonics can not be considered separately. One can expect that the motion of the bunch interacting with a large number of uncorrelated modes becomes random causing only diffusive growth of the bunch amplitude [4]. However, as illustrated in Fig.(1), at moderate amplitudes  $Y_0$ , the  $n$ -th harmonics rolls off with  $n$  and the strongest instability is due to the first harmonics.

Therefore, it is possible to consider, additional to the linear regime, two nonlinear stages of instability: first of moderate amplitudes, when instability is caused mostly by the lowest harmonics, and the second where higher harmonics can not be neglected. In this paper we consider the first case neglecting effect of all other harmonics of the nonlinear motion in the cloud but taking into account the amplitude dependence of the frequency  $\nu(Y_0)$ . It will be clear that the amplitudes remain relatively small all the time and, therefore, this case is the most interesting one.

#### 3.1 Free oscillations

Let us consider the initial stage of instability where  $Y = Y_f + \delta Y$  and the perturbation  $\delta Y$  is small compared with initial amplitude of free oscillations  $Y_f$ . Expression  $[Y - y_c]G(Y - y_c)$  in Eqs. (9),(10) can be expanded for small  $y_c$

$$[Y - y_c]G(Y - y_c) = Y_f G[Y_f] - y_c Q(z') + \delta Y Q(z'). \quad (21)$$

The first term leads to perturbation of a bunch by free oscillations of the cloud. This term is equivalent to some noise and can increase the beam emittance but has nothing to

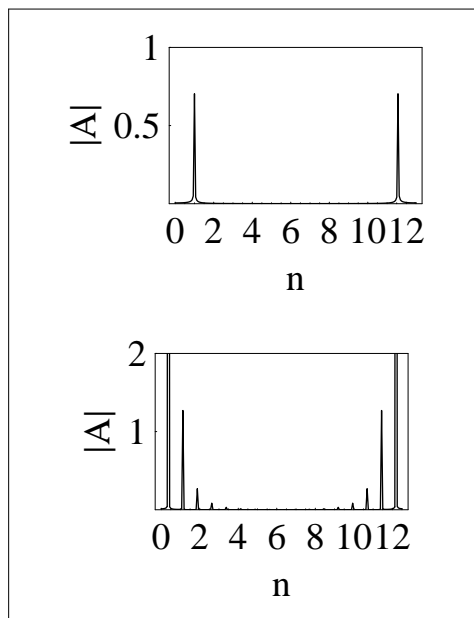


Figure 1: Spectrum of free oscillations of a nonlinear oscillator.  $G(Y) = 1/(1 + Y^2)$ , amplitude  $Y_0 = 0.1$  and  $Y_0 = 3.0$  for the upper and bottom panes, respectively.

do with the instability and can be omitted. The second term gives a betatron tune shift and can be included in the left-hand-side (LHS) of Eq. (9). Equations takes the form

$$\frac{\partial^2 y_c(\tau, \zeta)}{\partial \tau^2} + y_c(\tau, \zeta) = \Lambda \langle [YG[Y]] \rangle_{Y=Y(\tau, \zeta)}, \quad (22)$$

$$\frac{\partial^2 Y(\tau, \zeta)}{\partial \zeta^2} + Y(s, t)G[Y(s, t)] = y_c(\tau \zeta) \frac{\partial}{\partial Y} [YG[Y]]_{Y=Y(\tau, \zeta)}. \quad (23)$$

Neglecting higher harmonics of the motion, the solution can be found in the form of a single harmonics with the phase dependent on the amplitude  $Y_0$ ,

$$Y(\tau, \zeta) = Y_0 \cos(\psi), \quad \frac{\partial \psi}{\partial \zeta} = \nu(Y_0). \quad (24)$$

To find  $\nu(Y_0)$ , we consider the homogeneous equation

$$\frac{\partial^2 Y}{\partial \zeta^2} + YG(Y) = 0. \quad (25)$$

Substituting here Eq. (24), multiplying by  $\cos(\psi)$  and averaging over  $\psi$ , we found

$$\nu^2(Y_0) = 2 \int_{-\pi}^{\pi} \frac{d\psi}{2\pi} \cos^2(\psi) G[Y_0 \cos \psi]. \quad (26)$$

Note that  $\nu(0) = 1$ .

Let us take a simple form of  $G$  given by Eq. (8). Actually, we can use even simpler form,  $G(Y) = (1 + Y^2)^{-1}$ , re-scaling  $y_c$  and  $Y$  by the factor  $\kappa_0$ . Then, calculations give

$$\nu^2(Y_0) = \frac{2}{Y_0^2} \left(1 - \frac{1}{\sqrt{1 + Y_0^2}}\right). \quad (27)$$

The choice of  $G(Y)$  is not critical:  $\nu^2(Y_0)$  calculated using  $G(Y)$  in the form of Eq. (11) matches well with Eq. (58).

Comparison of  $\nu(Y_0)$  given by Eq. (58) with  $\nu(Y_0)$  determined from the solution of Eq. (25) with initial condition  $Y_0$  is shown in Fig. (2). Numerical  $\nu(Y_0)$  was found as the frequency at which the Fourier spectrum of the numerical solution of Eq. (25) at a given  $Y_0$  has maximum.

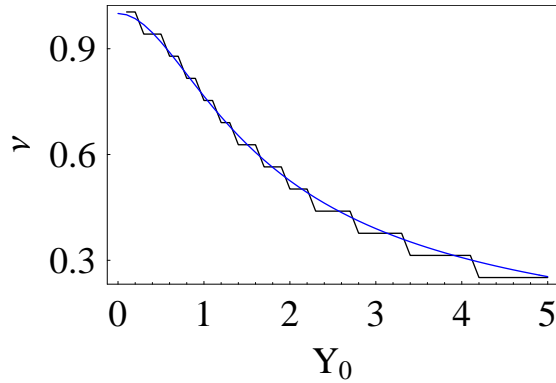


Figure 2: Comparison of  $\nu(Y_0)$  given by Eq. (58) (blue line) with  $\nu(Y_0)$  found numerically, see text.

### 3.2 Wake field

In the initial stage of instability when the perturbation  $\delta Y$  for a cloud particle is small, Eq. (23) in the approximation of a single harmonics for small  $y_c$  can be written as

$$\frac{\partial^2 Y(\tau, \zeta)}{\partial \zeta^2} + \nu^2(A)Y(\tau\zeta) = y_c(\tau, \zeta) \left(\frac{\partial}{\partial Y} [YG[Y]]\right)_{Y=Y(\tau, \zeta)}. \quad (28)$$

Eq. (28) has a formal solution

$$Y(\tau, \zeta) = Y_0 \cos(\psi) + \int_0^\zeta \frac{d\zeta'}{\nu(A_0)} \sin[\nu(A_0)(\zeta - \zeta')] y_c(\tau, \zeta') \left(\frac{\partial}{\partial Y} [YG[Y]]\right)_{Y=A_0 \cos[\psi(\zeta')]}, \quad (29)$$



where  $\partial\psi/\partial\zeta = \nu(A_0)$ . For  $\delta A \ll A_0$ , the RHS (right-hand-side) of Eq. (29) can be taken at  $A = A_0$ . Let us substitute result Eq. (29) in Eq. (22). The RHS of Eq. (22) takes the form

$$\int_0^\zeta d\zeta' y_c(\tau, \zeta') K(\zeta, \zeta'), \quad (30)$$

where

$$K(\zeta, \zeta') = \Lambda \left\langle \frac{1}{\nu(A_0)} \sin[\nu(A_0)(\zeta - \zeta')] G[Y_0] \left( \frac{\partial}{\partial Y} [YG[Y]]_{Y=Y_0} \right) \right\rangle. \quad (31)$$

Here  $Y_0 = A_0 \cos[\psi(\zeta)]$ .

Let us compare Eq.(30) with the definition of the wake field per unit length  $W$

$$\frac{\partial^2 y_c(s, z)}{\partial s^2} + \left( \frac{\omega_y^2}{c^2} \right) y_c(s, z) = \frac{r_e}{\gamma} \int dz' \lambda_b(z') W(z' - z) y_c(s, z') \quad (32)$$

where  $\lambda_b$  is the linear density of a bunch normalized to the bunch population  $\int dz \lambda_b(z) = N_b$ .

That gives

$$\begin{aligned} W(z - z') &= W_0 w(z - z'), \\ W_0 &= \frac{1}{\sigma_{c,y}} \frac{\Omega_b}{c} \left( \frac{\lambda_c}{\lambda_b(z')} \right) \frac{2}{\sigma_y(\sigma_x + \sigma_y)}, \\ w(z, z') &= \sigma_{c,y} \left\langle \frac{Q[A_0 \cos(\psi)]}{\nu(A_0)} G[A_0 \cos(\psi)] \sin[\nu(A_0)(\zeta - \zeta')] \right\rangle. \end{aligned} \quad (33)$$

Here

$$Q(Y_0) = \left( \frac{\partial}{\partial Y} [YG[Y]]_{Y=A_0 \cos[\psi]} \right). \quad (34)$$

The function  $w(z, z')$  is given by averaging over the phase  $\psi$  and the initial amplitude  $A_0$ . The average over  $A_0$  can be replaced by the averaging with the Gaussian distribution over initial  $Y_0$ . Going back to variable  $z$ , we get

$$w(z, z') = \int \frac{dY_0}{\sqrt{\pi}} e^{-\frac{Y_0^2}{2\sigma_{c,y}^2}} \frac{Q(Y_0)}{\nu(Y_0)} G[Y_0] \sin[\nu(Y_0) \frac{\Omega_y(z - z')}{c}]. \quad (35)$$

The factor  $\sigma_{c,y}$  is included in  $W_0$ . With such a definition,  $W_0$  depends on the average (1D) density of the cloud. Note that for the 1D averaging method,  $W_0$  has to be multiplied by the factor  $2\sigma_y/\sigma_{c,y}$ . In this case,  $W_0$  is proportional to the average density of the cloud  $n_c = \lambda_c/\sigma_c^2$ .

Calculations of  $w(z - z')$  as function of  $\Omega_y(z - z')/c$  depicted in Fig. (3) for  $\sigma = 5, 10$  and 20 show that the wake does not depend on the size of the cloud in agreement with

simulations [3]. The wake is a narrow-band wake  $W(z)/W_0 = w_0 \sin(\omega\zeta) e^{-\omega\zeta/2Q}$ , where  $\zeta = \Omega_y z/c$ . Eq. (35) allows us to calculate parameters  $w_0, \omega$ . It also gives the quality factor  $Q$  of the wake what is out of scope of the linear approximation [3]. The amplitude  $w_0$ , correction to the mode frequency  $\omega$ , and the quality factor  $Q$  are shown in Fig. (4).

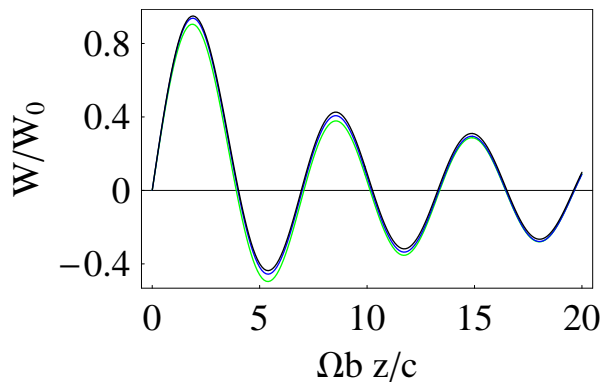


Figure 3: Wake field of e-cloud  $W(z)$  vs.  $\zeta = \Omega_y z/c$  determined by Eq. (35). The wake is calculated for three cases:  $\sigma_{c,y}/\sigma_y = 5$  (green line), 10 (blue) and 20 (red).

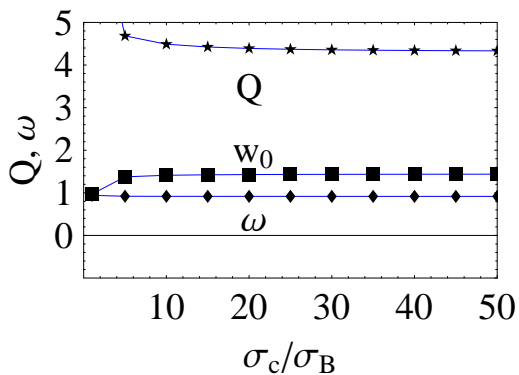


Figure 4: Parameters of the e-cloud wake vs. the size of the cloud  $\sigma_{c,y}/\sigma_y$ .

### 3.3 Numeric calculations

We compared our analysis with simple calculations of Eq. (9) and (10).

In calculations, Eq. (9) was replaced by the set of  $n_z$  equations for bunch slices with coordinates  $\zeta_k = (k - 1)\Delta$ ,  $k = 1, 2, \dots, n_z$

$$\frac{\partial^2 y_k(\tau)}{\partial \tau^2} + y_k(\tau) = \Lambda \langle [Y_k(\tau) - y_k(\tau)] G[Y_k(\tau) - y_k(\tau)] \rangle, \quad (36)$$

and solved with MATHEMATICA. Eq. (10) was replaced by the difference equation for cloud particles  $Y_i(\tau) = Y(\tau, \zeta_i)$ ,  $i = 2, 3, \dots, n_p$ ,

$$Y_{i+1}(\tau) = 2Y_i(\tau) - Y_{i-1}(\tau) - \Delta^2 [Y_i(\tau) - y_i(\tau)] G[Y_i(\tau) - y_i(\tau)]. \quad (37)$$

The function  $G(Y - y)$  was taken in the form  $G(Y) = (1 + Y^2)^{-1}$ .

The averaging over the cloud distribution was obtained distributing  $n_p$  particles uniformly over the initial offset  $-3 < Y_0 < 3$  (in units of the bunch transverse rms), calculating with Eq. (37) the offset for each of the particles, and replacing angular brackets in Eq. (36) with the sum over all  $n_p$  particles (divided by  $n_p$ ). Cloud particles in the ring (for all  $\tau$ ) had the offset  $Y_k^{(0)}$  at  $\zeta = 0$  when the first slice arrives at the location  $\tau$  of a particle. That defines  $Y_1(\tau) = Y_k^{(0)}$ ,  $k = 1, 2, \dots, n_p$ , and, by Eq. (36), describes the motion  $y_1(\tau)$  of the first slice of the bunch. The initial conditions for all slices were  $y_c(0, \zeta) = a_0$ , and  $(\partial y_c(\tau)/\partial \tau)_{\tau=0} = 0$ . Alternatively, the initial condition for slices can be chosen corresponding to the linear regime where  $y_c(\tau, \zeta) = a_0 \cos(\tau - \zeta)$ . Then,  $y_c(0, \zeta) = a_0 \cos(\zeta)$ , and  $(\partial y_c(\tau)/\partial \tau)_{\tau=0} = a_0 \sin(\zeta)$ . Results are not sensitive to the choice of the initial conditions for the slices.

Eq. (37) for  $Y_2(\tau)$  at  $\zeta = \delta$  takes the form

$$Y_2(\tau) = Y_1(\tau) - \frac{\Delta^2}{2} [Y_1(\tau) - y_1(\tau)] G[Y_1(\tau) - y_1(\tau)], \quad (38)$$

where we assume that the cloud particles are initially at rest,  $(dY_c(\tau)/d\zeta)_{\zeta=0} = 0$ , what gives  $Y_0 = Y_2$ . Eq. (38) defines  $Y_2(\tau)$ , and Eq. (36) gives  $y_2$ . The process is repeated for all slices of the bunch.

Results of numerical solution of Eqs. (8), (10) are shown in Fig. (5) for the cloud and Fig. (6) for a slice of the bunch. In Fig. (5) offsets of the cloud particles around the ring are taken at the moments corresponding to the interaction with a given slice (slices are numbered from the head to the tail of a bunch). At the moment corresponding to interaction with the first slice all offsets around the ring are given by the initial conditions. With time (i.e. for the following slices) particles start to oscillate with growing amplitude. However, the growth stops when the slice amplitude is large (and the amplitude is even decreases). The trajectory indicates presence of the higher order harmonics as it is clear from Fig.(7). However, the lowest harmonics gives the dominant contribution as it was assumed above.

Results show that initial exponential growth indeed takes place but for a very short period of time and then growth follows power law. At even larger time the behavior is quite complicated with periods of growth which can be followed by reduction of the size of the bunch.

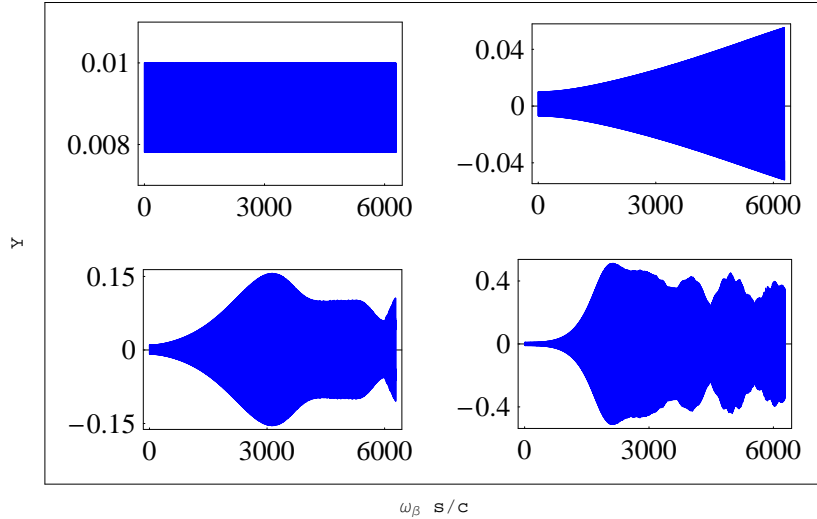


Figure 5: Offset of the cloud particles vs. position in the ring  $\tau = \omega_\beta^0 s/c$  taken at the moments corresponding to interaction with the slice number 2 (top, left), 4 (top right), 7 (bottom, left), and 20 (bottom right). Parameters are  $\Lambda = 0.012$ ,  $z_{max} = 3\pi$ ,  $a_0 = 0.01$ , 21 slice/bunch,  $n_p = 31$  distributed uniformly  $-1.0 < Y^0 < 1$ .

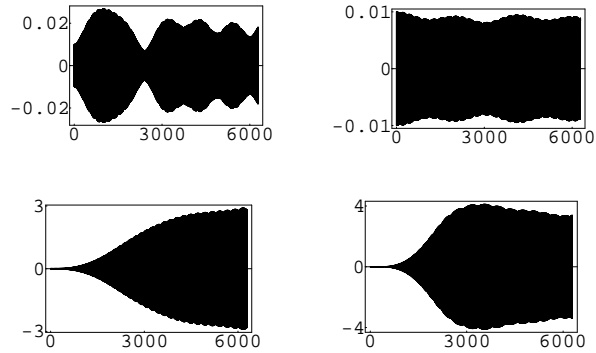


Figure 6: Offset of the bunch slices vs. position in the ring  $\tau = \omega_\beta^0 s/c$ . Contr-clockwise from the top right corner, slice number 4, 9, 16 and 20. Parameters are  $\Lambda = 0.012$ ,  $z_{max} = 3\pi$ ,  $a_0 = 0.01$ , 21 slice/bunch, cloud  $n_p = 31$  distributed uniformly  $-3.0 < Y^0 < 3.0$ .

## 4 Averaging

Although it is possible to solve Eqs. (9), (10) numerically directly, calculations are slow and has to be speed up. It is convenient to write Eqs. (9) and (10) in terms of the relative distance between bunch and cloud particles  $\xi(\tau, \zeta) = Y(\tau, \zeta) - y_c(\tau, \zeta)$ ,

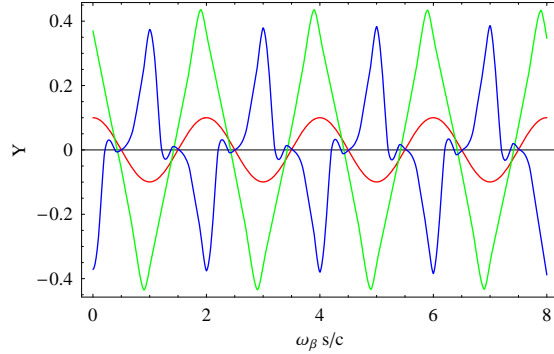


Figure 7: Trajectories of the cloud particles vs  $\tau = \omega_\beta^0 s/c$  taken at the moments of interaction with the slice number 20. Trajectories are depicted for three time intervals with the duration  $0 < \tau < 8\pi$  starting from  $\tau = 0$  (red line),  $\tau = 1000\pi$ , (green) and  $\tau = 1900\pi$  (blue). The amplitude of the trajectory in the first interval is multiplied by factor 10. Parameters are the same as for Fig. (5). Trajectories become un-harmonic at large  $\tau$  but the lowest harmonics dominates.

$$\begin{aligned} \frac{\partial^2 y_c(\tau, \zeta)}{\partial \tau^2} + y_c(\tau, \zeta) &= \Lambda \langle \xi(\tau, \zeta) G[\xi(\tau, \zeta)] \rangle, \\ \frac{\partial^2 \xi(\tau, \zeta)}{\partial \zeta^2} &= -\xi(\tau, \zeta) G[\xi(\tau, \zeta)] - \frac{\partial^2 y_c(\tau, \zeta)}{\partial \zeta^2}. \end{aligned} \quad (39)$$

We look for the induced solution in the form of a single harmonics

$$y_c(\tau, \zeta) = \frac{a(\tau, \zeta)}{2} e^{i(\zeta - \tau)} + c.c. \quad (40)$$

$$\xi(\tau, \zeta) = \frac{A(\tau, \zeta)}{2} e^{i(\zeta - \tau)} + c.c., \quad \xi'(\tau, \zeta) = i \frac{A(\tau, \zeta)}{2} e^{i(\zeta - \tau)} + c.c., \quad (41)$$

where prime means derivative over  $\zeta$ .

Equations for the complex amplitudes  $A$  and  $a$  can be obtained averaging fast oscillations assuming that amplitudes are slow functions of the arguments. The amplitude  $A$  satisfies equation

$$iA' - \frac{A}{2} + \frac{A}{2} \nu^2(|A|) = -\overline{y_c'' e^{-i(\zeta - \tau)}}, \quad (42)$$

where

$$\nu^2(|A|) = \overline{2 \cos^2(\psi) G(|A| \cos \psi)}, \quad (43)$$

and the bar denotes the averaging over the phase  $\psi$ .

Solution for  $y_c$  can be written in the form

$$y_c(\tau, \zeta) = a_0 \cos(\tau + \alpha_0) + \Lambda \int_0^\tau d\tau' \sin(\tau - \tau') \langle |A(\tau', \zeta)| \cos(\psi') G[|A(\tau', \zeta)| \cos(\psi')] \rangle \quad (44)$$

where  $\psi' = \psi(\tau', \zeta) = \zeta - \tau' + \arg A(\tau', \zeta)$ .

The average

$$\overline{y_c'' e^{-i(\zeta - \tau)}} = \left( \frac{\partial^2}{\partial \zeta^2} + 2i \frac{\partial}{\partial \zeta} - 1 \right) \overline{y_c e^{-i(\zeta - \tau)}} \quad (45)$$

is given in terms of

$$\frac{a(\tau, \zeta)}{2} = \overline{y_c e^{-i(\zeta - \tau)}} = \frac{a_0}{2} e^{-i\zeta - i\alpha_0} + \frac{i\Lambda}{4} \int_0^\tau d\tau' \langle A(\tau', \zeta) \nu^2(\tau', \zeta) \rangle. \quad (46)$$

That gives equations (the dot and prime mean derivatives over  $\tau$  and  $\zeta$ , respectively)

$$\begin{aligned} \dot{a}(\tau, \zeta) &= i \frac{\Lambda}{2} \langle A(\tau, \zeta) \nu^2(\tau, \zeta) \rangle, \\ A'(\tau, \zeta) + \frac{i}{2} (1 - \nu^2) A &= -\frac{i}{2} (1 - 2i \partial_\zeta - \partial_\zeta^2) a(\tau, \zeta). \end{aligned} \quad (47)$$

Equations can be combined in

$$\frac{\partial^2 A(\tau, \zeta)}{\partial \tau \partial \zeta} - \frac{i}{2} \frac{\partial}{\partial \tau} [(\nu^2(|A|) - 1) A] = \frac{\Lambda}{4} \left( 1 - 2i \frac{\partial}{\partial \zeta} - \frac{\partial^2}{\partial \zeta^2} \right) \langle (A(\tau, \zeta) \nu^2(\tau, \zeta)) \rangle. \quad (48)$$

The amplitude  $a_c(\tau, \zeta)$  is given by Eq. (46),

$$a(\tau, \zeta) = \frac{i\Lambda}{2} \int_0^\tau d\tau' \langle A(\tau', \zeta) \nu^2(\tau', \zeta) \rangle. \quad (49)$$

Integration here for large  $\tau$  takes into account that the cloud is refreshed at each turn. In the linear regime,  $a(\tau, \zeta)$  defined by Eq. (49) grows exponentially following growth of the amplitude  $A(\tau, \zeta)$ .

## 4.1 Linear regime, refined

Eq. (48) is different from Eq. (15) by the derivatives over  $\zeta$  in the RHS. Let us take them into account.

For small amplitudes  $|A| \ll 1$ ,  $\nu^2(\tau, \zeta) \simeq 1$  and Eq. (48) gives for  $f(\tau, \zeta) = \langle A(\tau, \zeta) \rangle$

$$\frac{\partial^2 f(\tau, \zeta)}{\partial \tau \partial \zeta} = \frac{\Lambda}{4} \left( 1 - 2i \frac{\partial}{\partial \zeta} - \frac{\partial^2}{\partial \zeta^2} \right) f(\tau, \zeta). \quad (50)$$

Solution of Eq. (50) can be obtained using Laplace transform over  $\tau$  and  $\zeta$ ,

$$f(\tau, \zeta) = e^{-2iu} \int_{-\infty}^{\infty} \frac{dq}{2\pi i} \frac{g(q)}{q} e^{i(\zeta-u)q - i\frac{u}{q}}, \quad (51)$$

where  $u = \Lambda\tau/4$  and

$$g(q) = \int_{-\infty}^{\infty} d\zeta \frac{\partial f(0, \zeta)}{\partial \zeta} e^{-iq\zeta}. \quad (52)$$

Expanding  $g(q)$  over  $q$ , and using generating function for Bessel functions

$$e^{\frac{z}{2}(w - \frac{1}{w})} = \sum_{n=-\infty}^{\infty} w^n J_n(z), \quad (53)$$

we obtain solution of Eq. (50)

$$f(\tau, \zeta) = e^{-2iu} \sum_n g_n \left(\frac{u - \zeta}{u}\right)^{n/2} J_n(2\sqrt{u(u - \zeta)}), \quad (54)$$

where the coefficients  $g_n$  are determined by the initial conditions. It is easy to check that each term in the series satisfies Eq. (50) exactly. We dropped another solution proportional to Bessel function of the second kind which is singular either at  $\zeta = u$  or at  $u = 0$ .

Note that the solution oscillates for  $u > \zeta$  and  $f$  grows exponentially at large  $\zeta > u \gg 1$ . Let us remind that  $\zeta$  for the cloud plays role of time. The result of Eq. (19) can be obtained from Eq. (54) replacing  $(u - \zeta)$  by  $(-\zeta)$  in the argument of Bessel function.

Solution of the form of Eq. (54) was obtained before [9] and interpreted as the BNS damping due to spread of cloud frequencies. In this paper it was demonstrated that the growth can be totally suppressed for very special initial conditions. We do not consider this question here because in reality any fluctuations would induce exponential growth for  $u < \zeta$ .

Consider, for example, the case where all  $g_n = 0$  except  $g_0$ . At the moment  $\zeta = 0$  when a particle situated at  $u > 0$  in the ring interacts with the head of the bunch solution is generated by the initial conditions

$$\begin{aligned} f(\tau, 0) &= g_0 e^{-2iu} J_0(2u), & \frac{\partial f(0, \zeta)}{\partial \zeta} &= 0, \\ \left(\frac{\partial f(\tau, \zeta)}{\partial \zeta}\right)_{\zeta=0} &= g_0 e^{-2iu} J_1(2u). \end{aligned} \quad (55)$$

Eq. (55) allows us to verify applicability of the averaging method. The latter implies that the amplitude  $f(\tau, \zeta)$  is a slow function compared to the factor  $e^{i(\zeta-\tau)}$ . Hence, the variation of  $f(\tau, \zeta)$  has to be small on the scale of  $\tau \simeq 1$  and  $\tau \simeq 1$ . Because the typical

scale of variation of  $f(\tau, \zeta)$  is of the order of  $2\sqrt{u\zeta} = \sqrt{\Lambda\zeta\tau}$ , the averaging is applicable if  $\Lambda \ll 1$ .

Eq. (55) can be used as initial conditions for Eq. (50) and can serve us to check numeric calculations in the nonlinear case.

Eq. (54) shows that small initial oscillations of a bunch excite exponentially growing oscillations of the cloud for  $\zeta > u$ . This condition in usual units means

$$s < s_{cr}, \quad s_{cr} = \frac{4\Omega_y}{\Lambda\omega_y} z. \quad (56)$$

For PEP-II B-factory, where the 2.5 Amp. positron beam in the  $C = 2.2$  km ring has the average rms  $\sigma_{x,y} = \{1200, 200\} \mu m$ ,  $\sigma_z = 1$  cm, energy  $E = 3.1$  GeV, and the tune  $Q_y \simeq 36$ . Taking  $n_{cl} = 10^7 \text{ cm}^{-3}$ , we get  $\Omega_e = 66$ . GHz,  $\Lambda = 0.005$ , and  $s_{cr} = 16 \gg C$  km. This estimates show that, for realistic parameters, the linear approximation predicts exponential growth over the ring except a very thin slice in the head of the bunch [10]. That is true also for the parameters of the Super-B factory for the same density of the cloud and for the fast ion instability where the coasting beam approximation corresponds to very long bunches.

Fig. (8) shows transition from oscillations for small  $\zeta$  to exponential growth for  $\zeta > u$  in the linear regime. The growth starts later for larger  $\tau$  as it is predicted by Eq. (54).

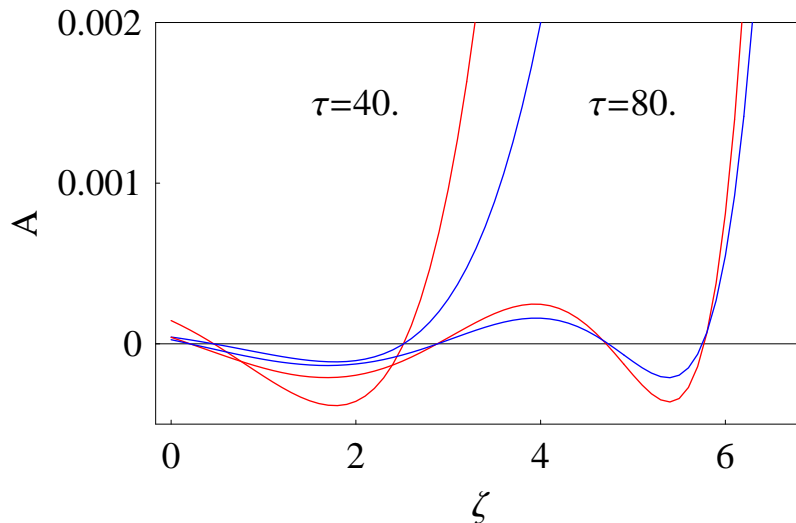


Figure 8: Transition from oscillations at  $\zeta < u$  to exponential growth at the locations  $\tau = 40$  and  $\tau = 80$ . Variation of  $Re(A)$  (red) and  $Im(A)$  (blue). The same initial and boundary conditions correspond to the exponential regime. Exponential growth starts later for larger  $\tau$ . Parameters:  $\Lambda = 0.3$ ,  $z_{max} = 8.0$ ,  $y_0 = 0.001$ .



## 4.2 Growth in the quasi-linear regime

Let us neglect derivatives over  $\zeta$  in the RHS of Eq. (47). That gives equations

$$\dot{a} = i\frac{\Lambda}{2}\langle\nu^2(|A|)A\rangle, \quad A'(\tau, \zeta) = -\frac{i}{2}(1 - \nu^2)A - \frac{i}{2}a, \quad (57)$$

where  $\nu$  is given by Eq. (58),

$$\nu^2(|A|) = \frac{2}{|A|^2} \left(1 - \frac{1}{\sqrt{1 + |A|^2}}\right). \quad (58)$$

For small  $A$ ,  $\nu \simeq 1 - \frac{3}{8}|A|^2$ .

The formal solution for  $A$  takes the form

$$A(\tau, \zeta) = A_0 e^{-\frac{i}{2}\Phi(\tau, \zeta)} - \frac{i}{2} \int_0^\zeta d\zeta' a(\tau, \zeta') e^{-\frac{i}{2}[\Phi(\tau, \zeta) - \Phi(\tau, \zeta')]}, \quad (59)$$

where  $\Phi(\tau, z) = \int_0^z dz' (1 - \nu^2(\tau, z'))$ , and  $A_0$  is defined by the initial conditions.

Substituting Eq. (59) in the equation for  $\dot{a}$ , neglecting free oscillations term proportional to  $A_0$ , and approximating  $\Phi(\tau, \zeta) - \Phi(\tau, \zeta') \simeq (\zeta - \zeta')(1 - \nu^2)$ , we get the following equation:

$$\begin{aligned} \dot{a}(\tau, \zeta) &= - \int_0^\zeta dz' K(z - z') a(\tau, z'), \\ K(z - z') &= -\frac{\Lambda}{4} \langle \nu^2 e^{-\frac{i}{2}(1 - \nu^2)(z - z')} \rangle. \end{aligned} \quad (60)$$

In the quasi-linear regime, the amplitude  $A$  can be approximated by the initial conditions. In this case,  $\Phi(\tau, \zeta) \simeq \Phi(\zeta)$  and Eq. (60) can be solved analytically. Solution is given in Appendix 3. The result is, essentially, the same as in the linear case,

$$a(s, z) = \frac{a_0}{\sqrt{2\pi}} \frac{1}{(\Lambda_{eff}\tau\zeta)^{1/4}} e^{\sqrt{\Lambda_{eff}\tau\zeta}}, \quad (61)$$

but with  $\Lambda_{eff}$  instead of  $\Lambda$ , where  $\Lambda_{eff} = \Lambda\langle\nu^2\rangle$ .

At large amplitudes  $A$  of particles of the cloud,  $\Lambda_{eff}$  decreases, see Fig. (9), what stops the exponential growth of the linear approximation.

## 5 Transition to large amplitudes

Exponential growth of the linear regime leads to large amplitudes of oscillations. For large  $y_c$ , the relative offset  $\xi = Y - y_c$  is also large, and the terms  $\xi G$  in the RHS of Eq. (39) go to zero. In this limit,  $\xi = -y_c$ . Comparing that with the definition of  $\xi$  one can expect that  $Y \rightarrow 0$  for particles of the cloud and large amplitude betatron oscillations

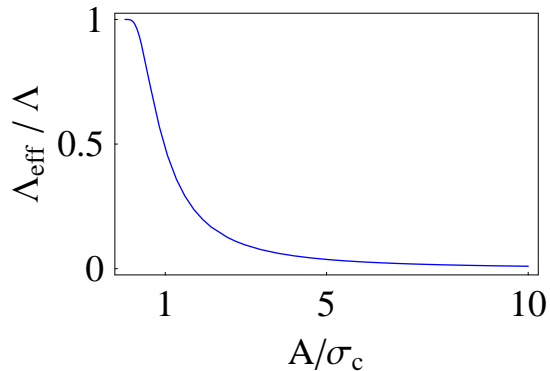


Figure 9: Parameter  $\Lambda_{eff}/\Lambda$  as function of the amplitude of the cloud oscillations.

for the beam. More accurately, we note that because  $G[y_c]$  decreases as  $(1/y_c)^2$  at large amplitude of oscillations  $y_c$ , the RHS in Eq. (39) is small almost all the time except short periods when  $y_c$  is close to zero, see Fig. (10).

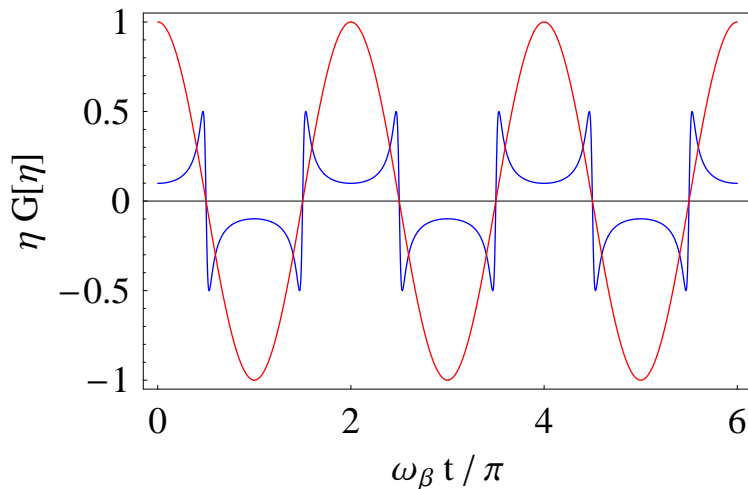


Figure 10: The RHS of Eq. (62) (blue line) is a series of kicks at the moments when  $y_c = a \cos[\tau]$  (red line) is small. In the illustration  $a = 10.0$ .

The beam-cloud interaction takes the form of series of kicks and averaging over the phase of oscillations used at small amplitudes does not work well. We use another approach utilizing that the asymptotic regime corresponds to small offsets  $Y$ , and expanding  $\xi G[\xi]$  over  $Y$ . Equations take the form

$$\frac{\partial^2 Y(\tau, \zeta)}{\partial \zeta^2} = y_c(\tau, \zeta) G[y_c(\tau, \zeta)] - Y(\tau, \zeta) \left( \frac{\partial}{\partial y_c} [y_c G[y_c]] \right)_{\tau, \zeta}. \quad (62)$$

$$\frac{\partial^2 y_c(\tau, \zeta)}{\partial \tau^2} + y_c(\tau, \zeta) = -\Lambda \langle y_c G[y_c] + \Lambda Y(\tau, \zeta) \left( \frac{\partial}{\partial y_c} [y_c G[y_c]] \right) \rangle. \quad (63)$$

Eq. (62) with the initial conditions  $Y(\tau, 0) = Y_0$ ,  $(dY(\tau, \zeta)/d\zeta)_{\zeta=0} = P_0$  has a formal solution  $Y(\tau, \zeta) = Y_0 + P_0 \zeta + \delta Y(\tau, \zeta)$ ,

$$\delta Y(\tau, \zeta) = \int_0^\zeta d\zeta' (\zeta - \zeta') \left\{ R(\tau, \zeta') - \frac{\partial R(\tau, \zeta')}{\partial y_c(\tau, \zeta')} Y(\tau, \zeta') \right\}, \quad (64)$$

where

$$R(\tau, \zeta) = y_c(\tau, \zeta) G[y_c(\tau, \zeta)]. \quad (65)$$

For small  $\delta Y$ , averaging removes the free oscillation terms and iteration gives

$$\begin{aligned} \langle Y(\tau, \zeta) \rangle &= \int_0^\zeta d\zeta' (\zeta - \zeta') R(\tau, \zeta') \\ &- \int_0^\zeta d\zeta' \int_0^{\zeta'} d\zeta'' (\zeta - \zeta') (\zeta' - \zeta'') \frac{\partial R(\tau, \zeta')}{\partial y_c(\tau, \zeta')} R(\tau, \zeta''). \end{aligned} \quad (66)$$

Let us substitute that in Eq. (63). The term  $\Lambda y_c G(y_c)$  in the RHS of Eq. (63) perturbs betatron motion but is not related to the instability. We discuss effect of this term in the next subsection. Retaining the second term the RHS of Eq. (63) we get

$$\frac{\partial^2 y_c(\tau, \zeta)}{\partial \tau^2} + y_c(\tau, \zeta) = \Lambda \langle Y(\tau, \zeta) \left( \frac{\partial y_c G[y_c]}{\partial y_c} \right)_{y_c \rightarrow y_c(\tau, \zeta)} \rangle. \quad (67)$$

We look for the solution of Eq. (67) in the form  $y_c(\tau, \zeta) = a(\tau, \zeta) \cos(\tau - \zeta)$ . Multiplying both sides of equation by  $\sin(\omega_s/c - \Omega_b z/c)$  and averaging over  $s$ , we get equation for the slow amplitude  $a(s, z)$ . Neglecting the correction of the second line of Eq. (66), we get

$$\frac{\partial a(\tau, \zeta)}{\partial \tau} = -\Lambda \overline{\langle \sin(\tau - \zeta) \left( \frac{\partial R[y_c(\tau, \zeta)]}{\partial y_c(\tau, \zeta)} \right) \int_0^\zeta d\zeta' (\zeta - \zeta') R[y_c(\tau, \zeta')] \rangle}. \quad (68)$$

For  $G(Y) = (1 + Y^2)^{-1}$ , Eq. (68) takes the form

$$\frac{\partial a(\tau, \zeta)}{\partial \tau} = -\Lambda \int_0^\zeta d\zeta' (\zeta - \zeta') \overline{\langle \sin(\tau - \zeta) \left( \frac{1 - y_c^2(\tau, \zeta)}{[1 + y_c^2(\tau, \zeta)]^2} \right) \frac{y_c(\tau, \zeta')}{1 + y_c^2(\tau, \zeta')} \rangle}. \quad (69)$$

Here  $y_c(\tau, \zeta) = a \cos(\psi)$ ,  $y_c(\tau, \zeta') = b \cos(\psi + \alpha)$ , where  $a = a(\tau, \zeta)$ ,  $b = a(\tau, \zeta')$ , and  $\psi = \tau - \zeta$ ,  $\alpha = \zeta - \zeta'$ .

We want to average the RHS of Eq. (69) over  $\psi$  and fast oscillations in  $\alpha$ . The amplitudes  $a$ ,  $b$  are slow functions of arguments and can be considered as constants for the averaging. Eq. (69) takes the form

$$\frac{\partial a(\tau, \zeta)}{\partial \tau} = -\Lambda \int_0^\zeta d\zeta' \langle \alpha \sin(\psi) \left( \frac{1 - a^2 \cos^2(\psi)}{[1 + a^2 \cos^2(\psi)]^2} \right) \frac{b \cos(\psi + \alpha)}{1 + b^2 \cos^2(\psi + \alpha)} \rangle_{\psi, \alpha}. \quad (70)$$

Having in mind the following averaging over  $\psi$ , it is suffice to replace the average

$$\left\langle \frac{\alpha b \sin(\psi) \cos(\psi + \alpha)}{1 + b^2 \cos^2(\psi + \alpha)} \right\rangle_{\alpha}. \quad (71)$$

by

$$-\sin^2(\psi) \int_0^{2\pi} \frac{d\alpha}{2\pi} \frac{b \alpha \sin(\alpha)}{1 + b^2 \cos^2(\psi + \alpha)} = \frac{b \sin^2(\psi)}{2(1 + b^2/2)} \int_0^\pi \frac{d\alpha \sin(\alpha)}{1 + d^2 \cos(2\psi + 2\alpha)}, \quad (72)$$

where  $d^2 = b^2/(b^2 + 2)$ .

For large  $b \gg 1$ , the integral in Eq. (72) can be approximated as

$$\int_0^\pi \frac{d\alpha \sin(\alpha)}{1 + d^2 \cos(2\psi + 2\alpha)} \simeq \frac{\pi b}{2} \left\{ |\cos(\psi)| - \frac{2}{\pi b} - \frac{1}{\pi b} \sin(\psi) \ln\left(\frac{1 - \sin \psi}{1 + \sin \psi}\right) \right\}. \quad (73)$$

Now we can calculate the average over  $\psi$ . Neglecting small terms  $o(1/b)$ , the angular brackets in Eq. (70) is given by the integral

$$\int_0^{\pi/2} d\psi \sin^2(\psi) \cos(\psi) \left( \frac{1 - a^2 \cos^2(\psi)}{[1 + a^2 \cos^2(\psi)]^2} \right) \quad (74)$$

For large  $a \gg 1$ , the integral is

$$-\frac{1}{a^2} (\ln(a) - 1). \quad (75)$$

Eq.(70) takes the form

$$\frac{\partial a(s, z)}{\partial \tau} = \frac{\Lambda \zeta}{a^2} (\ln a - 1). \quad (76)$$

Eq. (76) has the approximate solution

$$a(s, z) \propto [\Lambda \zeta (\tau - \tau_0)]^{1/3}. \quad (77)$$

where  $\tau_0$  is an arbitrary constant.

The amplitude in the asymptotic of large  $\tau$  grows but only as  $\tau^{1/3}$ . However, as it is clear from derivation, this behavior is limited to large but moderate  $\tau$ . At even larger  $\tau$  the power can be different from 1/3 as it is shown below.

We compared Eq. (77) with calculations based on Eq. (9) and (10). The typical parameters used in simulations were  $a_0 = 0.01$ ,  $Y_0 = 0.01$ ,  $\Lambda = 0.012$ ,  $\tau_{max} = 6280$ , number of slices  $n_z = 21$ , number of oscillations of the cloud particle per bunch  $\zeta_{max} = \Omega_b z_{max}/c = 3\pi$ .

Example of numeric solution of Eqs. (9), (10) is given in Fig. (11), where trajectory of a the last slice  $y(t, z_{max})$  interacting with the cloud is compared with the estimate Eq. (77).

Comparison shows that after initial fast growth the amplitude increases much slower following Eq. (77). Transition from exponential regime to the power low regime corresponds to the bunch amplitude of the order of one (in units of the beam rms  $\sigma_b$ ).

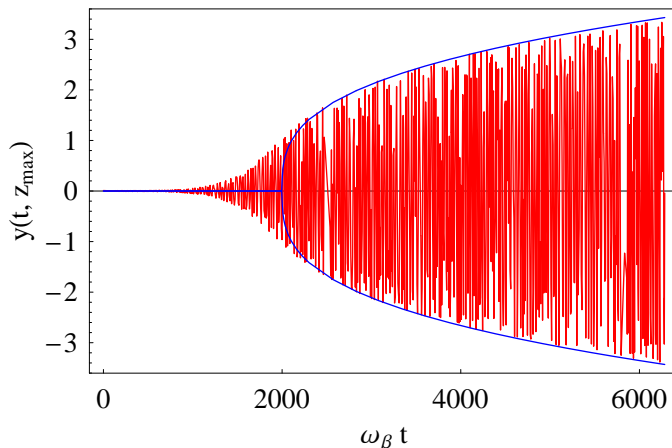


Figure 11: Trajectory of a the last slice  $y(s, z_{max})$  (shown in red). Trajectory is calculated numerically, see text. Result is compared with asymptotic behavior of Eq. (77) (blue line) calculated as  $a(s, z) = a[\Lambda\zeta_{max}(\tau - \tau_0)]^{1/3}$  for  $\tau > \tau_0$ . The fitting parameters are  $\tau_0 = 2000$  and  $a = 0.44$ . Transition from exponential regime to the power low regime takes place when amplitude is of the order of one.

## 6 Effect of the cloud on optics

So far we neglected the term  $\lambda_0 y_c G(y_c)$  in the RHS of Eq. (63). With this term, equation for the betatron oscillations takes the form

$$\frac{\partial^2 y_c(s, z)}{\partial s^2} + \left(\frac{\omega_\beta^0}{c}\right)^2 y_c(s, z) = -\lambda_0 y_c G(y_c). \quad (78)$$

In the linear approximation,  $G \rightarrow 1$ , the RHS changes the betatron frequency to  $Q_\beta = Q_\beta^0 + \Delta Q_\beta$ , where the linear tune shift

$$\Delta Q_\beta = \frac{\Lambda}{2} Q_\beta^0 \beta = \frac{r_e}{\gamma} \frac{\lambda_c}{\sigma_y(\sigma_x + \sigma_y)} \left(\frac{R^2}{2Q_y^0}\right) \quad (79)$$

is proportional to the average machine radius  $R$  squared and can be quite large for large machines.

The tune measurements are carried out, in reality, always when the beam-cloud interaction is in the nonlinear regime. Let us look for the solution of Eq. (78) for dimensionless  $y_c$

$$y_c''(\tau) + y_c(\tau) = -\Lambda y_c G(y_c) \quad (80)$$

in the form

$$y_c = y_0 \cos(\nu\tau) + \frac{y_0'}{\nu} \sin(\nu\tau) = \sqrt{\frac{2J}{\nu}} \cos(\nu\tau - \phi). \quad (81)$$

Here emittance (adiabatic invariant)  $J = (2/\nu)\epsilon^2$  is defined by the amplitude of oscillations  $\epsilon$ ,  $\epsilon^2 = y_0^2 + (y_0'/\nu)^2$ .

Substituting  $y_c$  in terms of  $J$  in Eq. (80) and averaging over fast oscillations, we get

$$\nu^2 = 1 + 2\Lambda \langle \cos^2(\psi) G[\sqrt{\frac{2J}{\nu}} \cos(\psi)] \rangle_\psi. \quad (82)$$

For a simple model  $G(Y) = (1 + Y^2)^{-1}$ ,

$$\nu^2(\epsilon) = 1 + \frac{2\Lambda}{\epsilon^2} \left(1 - \frac{1}{\sqrt{1 + \epsilon^2}}\right). \quad (83)$$

For small amplitudes  $\epsilon \rightarrow 0$ , Eq. (83) reproduces result of the linear approximation,  $\nu^2 \rightarrow \nu_0^2 = 1 + \Lambda$ . The quantity  $\Delta Q_\beta/Q_\beta = (\nu - 1)$  is shown in Fig. (12) as function of the dimensionless amplitude of oscillations  $\epsilon$ . It starts at  $\Lambda/2$  at small amplitudes and rolls off to zero as  $\Lambda/\epsilon^2$ .

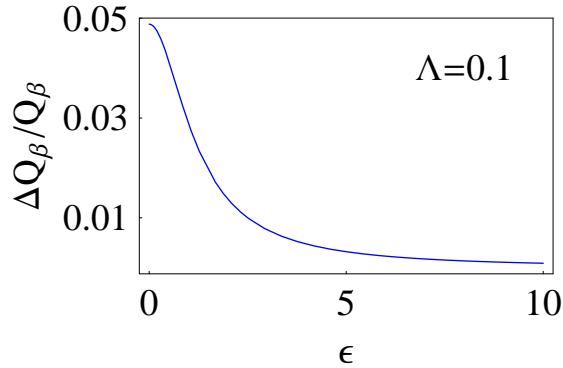


Figure 12: Dependence of the tune shift  $\Delta Q_\beta/Q_\beta^0$  on the dimensionless amplitude of the beam oscillations  $\epsilon$ . Parameter  $\Lambda = 0.1$ .

Note that the beam emittance decreases with amplitude of oscillations as

$$\frac{J(\epsilon)}{J(0)} = \frac{\nu}{\nu_0}. \quad (84)$$

## 7 Nonlinear regime

Exponential growth can be stopped only due to the nonlinearity of the motion. Eqs. (47) (we use here  $u = \Lambda\tau/4$ ),

$$\begin{aligned}\dot{a}(u, \zeta) &= 2i\langle A(u, \zeta)\nu^2(u, \zeta)\rangle, \\ A'(u, \zeta) + \frac{i}{2}(1 - \nu^2)A &= -\frac{i}{2}(1 - 2i\partial_\zeta - \partial_\zeta^2)a(u, \zeta),\end{aligned}\quad (85)$$

can be simplified in the asymptotic of large  $|A| \gg 1$ . First, in this case, parameter  $\mu^2 \simeq 2/|A|^2$  and becomes small  $\mu \ll 1$ . Second, as it was shown above, the terms with derivatives in the RHS of the second Eq. (85) are not important except for very large distances where the tune spread reduces the growth (exponential in the linear case). We can expect, that for  $\zeta \gg 1$  it is true also in the nonlinear case and these terms can be neglected. Third, assuming that the asymptotic behavior of  $A$  is not sensitive to the initial conditions, we can drop the angular brackets in Eq. (85). Therefore, for  $|A| \gg 1$  and  $\zeta \gg 1$ , Eq. (85) can be simplified and take the form

$$\begin{aligned}\dot{a}(u, \zeta) &= 4i\frac{A(u, \zeta)}{|A(u, \zeta)|^2}, \\ A'(u, \zeta) + \frac{i}{2}A &= -\frac{i}{2}a(u, \zeta).\end{aligned}\quad (86)$$

Let us define new amplitudes  $\alpha$  and  $B$ ,

$$a(u, \zeta) = \alpha(u)e^{-i\zeta/2}, \quad A(u, \zeta) = -iB(u)e^{-i\zeta/2}, \quad (87)$$

transforming Eq. (86) to

$$\dot{\alpha}(u, \zeta) = 4\frac{B(u, \zeta)}{|B(u, \zeta)|^2}, \quad B'(u, \zeta) = \frac{1}{2}\alpha(u, \zeta). \quad (88)$$

Equations are real and, in the asymptotic, we can assume that  $\alpha$  and  $B$  are also real. Combining Eq. (88), we get

$$\frac{\partial^2 B(u, \zeta)}{\partial u \partial \zeta} = \frac{2}{B(u, \zeta)}. \quad (89)$$

Solution of Eq. (89) can be found similarly to Section 2.1 in the form  $B(u, \zeta) = f(x)$  where  $x = u\zeta$ . The function  $f$  satisfies

$$f \frac{d}{dx} \left( x \frac{df}{dx} \right) = 2, \quad (90)$$

and has solution  $f(x) = \sqrt{8x}$ . Hence,

$$a(u, \zeta) = 2\sqrt{\frac{2u}{\zeta}} e^{-i\zeta/2}, \quad A(u\zeta) = -2i\sqrt{2u\zeta} e^{-i\zeta/2}, \quad (91)$$

and  $|A| = \sqrt{8u\zeta}$ . It is easy to see that the result Eq. (91) justifies assumptions assumed in derivation provided  $u \gg 1$  and  $\zeta \gg 1$ .

Solution Eq. (91) agrees with numeric solution of Eqs. (47). Eq. (85) can be solved in turns. We replace the second equation by the difference equation for the amplitudes  $A(u, \zeta_j)$  of the cloud particles at the location  $u$  at the moment of interaction with the bunch slice  $j$ , i.e. at  $z_j = \Delta z(j-1)$ ,  $j = 1, 2, \dots, N_z$ . We start calculations defining  $A(u, 0) = A_0$  around the ring at the moment when the head of the bunch comes to the location  $u$ . Distribution of  $A_0$  for  $n_p$  particles corresponds to the distribution of the cloud particles at that moment. Then, solution of the first of Eqs. (85) defines  $a(u, 0)$  for all location  $u$ . In the next step, the difference equation can be used to obtain  $A(u, \Delta\zeta)$  and, then, the first equation defines the amplitude  $a(u, \Delta\zeta)$  of the second slice, etc. Calculations are carried out for the array of  $n_p$  cloud particles and the averaging (denoted by the angular brackets in Eqs. (85)) is obtained calculating the sum over all particles weighted by the initial distribution.

Results obtained in this way are shown in Figs. (14)-(16). Fig. (13) shows variation of the amplitude of the last slice vs. time  $u$ . The red and blue lines correspond to  $n_p = 3$  and  $n_p = 21$ , respectively. The amplitudes of all slices at the end of the run  $u_{max} = 49.5$  are shown in Fig. (14). Both figures show that the results are not very sensitive to  $n_p$  what allows us to use low  $n_p$  saving CPU time. That is also true for the amplitudes  $A$  of different particles in the cloud. The amplitudes  $A$  at  $u = u_{max}$  are shown in Fig. (15) for all  $n_p = 21$  cloud particles after interaction with the last slice  $z = z_{max}$ . Variation of the amplitude in Fig. (15) is relatively small. Dependence of the average amplitude of the cloud particles on the location  $u$  around the ring at the moment of interaction with the last slice of a bunch is shown in Fig. (16). The growth of the amplitude is fitted with the  $\sqrt{u - u_0}$  dependence for  $u > u_0$  where  $u_0$  is fitting parameter.

At the moderate  $u$  these results agree with numeric simulations of transition from the exponential growth to the growth following a power law. However, at large  $u$  results contradict to direct numeric simulations depicted in Fig. (5) and Fig. (6) where amplitudes of the bunch and of the cloud go asymptotically to saturation.

Possible explanation for the disagreement can be found in the form of solution Eq. (91), where  $A$  oscillates as  $e^{-i\zeta/2}$ . Such oscillation contradicts the basic assumption of the averaging method that the amplitude is a slow function compared to the factor  $e^{i\zeta}$ . We can expect that due to the factor  $e^{-i\zeta/2}$  different modes at large  $u$  are coupled and interfere destructively.

Therefore, the averaging method is limited only to moderate time intervals describing transition from the exponential regime to saturation.



## 8 Comment on the FII

Since the pioneering work of Zenkevitch and Koshkarev [11] it is known that ions generated by and interacting with the beam can drive the beam instability. Their analysis predicts resonances at the revolution harmonics  $n\omega_0$  within the interval  $\omega_\beta < n\omega_0 < \omega_\beta + \Omega_b$ . The growth rate of instability is strongest at the maximum  $n$  in this interval. Such result is valid for small machines, where resonances are well separated. In large machines, where  $\omega_0$  is small and the growth rate is large, the resonances may overlap. The instability in this case does not have a resonance character [2] and is called the fast ion instability (FII). The growth rate of FII instability [2] can be described in the same way as for electron cloud instability. The differences are minor. First of all, for the large ion clearing gap in the bunch train, the ion density increases along the train. As a result, the factor  $z$  in Eq. (19) is replaced by  $z^2$  provided the growth rate is expressed in terms of the ion production rate. Secondly, the transverse rms of the initial ion cloud is the same as for the beam assuming that ions are produced mostly in collisions with the residual gas. However, this changes do not affect the analysis presented in this paper.

As we show above, the instability, except for a very short initial period, is stabilized by the nonlinearity of motion. Hence, the relatively weak but high frequency feedback system which can affect the head and the tail of a bunch in a different way can be effective in suppressing the instability. Although such system exists for proton long bunches, its feasibility still has to be demonstrated for short bunches of electron machines. It would be important also to include the synchrotron motion into consideration. The latter interferes with the longitudinal modulation of a bunch imposed by the instability and may further stabilize the instability.

## 9 Conclusion

We presented analytic study of the single bunch electron cloud instability. Results are obtained in 1D case and for the simplified form of the beam-cloud interaction. However, the approach can be easily generalized to the realistic 2D case with Bassetti-Erskine interaction and for study of the fast ion instability. Results of the linear approximation are refined but, for realistic parameters, the difference with the well known results is insignificant. We extend analysis to the nonlinear case what is important for understanding of the saturation mechanism of the instability and for prediction the asymptotic amplitude of oscillations. Some analytic results are obtained considering intermediate quasi-linear regime including the  $Q$ -factor of the e-cloud wake field and character of the amplitude growth in the transition. We use the averaging method obtaining equations of motion applicable to the transition regime of instability. Numeric solution of these equations is faster than direct solution of the equation of motion, typically by an order of magnitude. However, it seems that the averaging method does not lead to saturation at very large time.

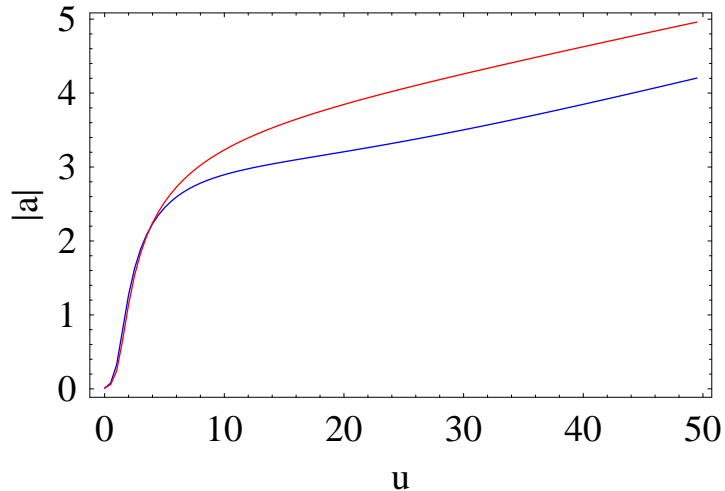


Figure 13: Amplitude of the last slice vs time  $u$ . Results are very close for the number of cloud particles  $n_p = 3$  (red line) and  $n_p = 21$  (blue line). Cloud particles are initially uniformly distributed within  $-1 < Y_0 < 1$ , number of slices  $N_z = 101$ , total length  $z_{max} = 10$ , the initial offset of all slices  $y_0 = 0.01$ .

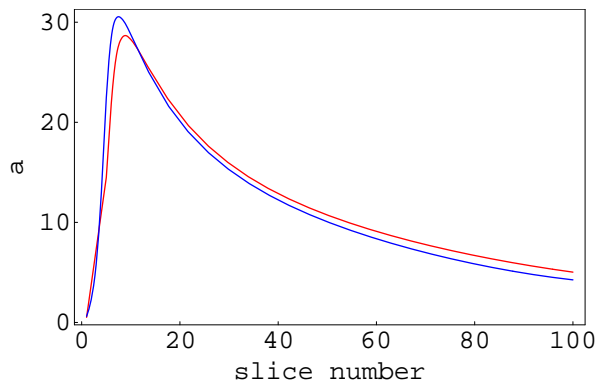


Figure 14: Amplitudes of bunch slices at the end of the run, at  $u_{max} = 49.5$ . All parameters and notations are the same as in Fig. (13).

## 9.1 Acknowledgement

I thank G. Stupakov for useful discussions and help.

Work supported by Department of Energy contract DE-AC03-76SF00515.

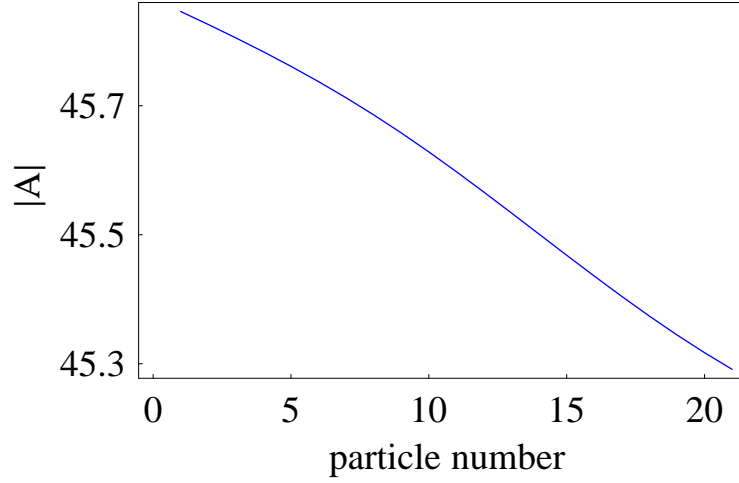


Figure 15: Amplitudes of the  $n_p = 21$  cloud particles after interaction with the last slice in the bunch at the location  $u = u_{max}$ . Variation of the amplitudes is relatively small. Other parameters are the same as in Fig. (13).

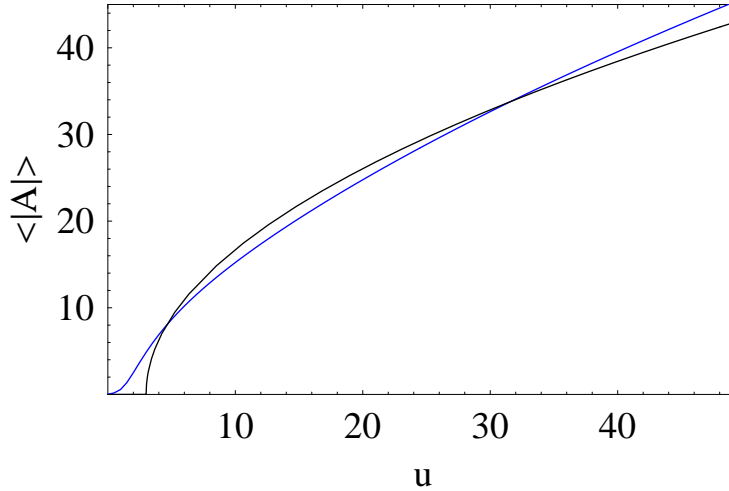


Figure 16: Averaged amplitude  $\langle |A| \rangle$  of cloud particles vs. location in the ring  $u$ . Number of slices  $n_z = 101$ , the total bunch length  $z_{max} = 10$ . Dependence is fitted with  $\langle |A| \rangle = 2\sqrt{z_{max}(u - u_0)}$  for  $u > u_0$  with one fitting parameter  $u_0$ . Other parameters are the same as in Fig. (13).

## References

- [1] K. Ohmi, Beam and Photoelectron Interaction in positron storage rings, KEK preprint 94-198, February 1995

- [2] T.O. Raubenheimer, F. Zimmermann, PR E52, No. 5 (1995) 5487
- [3] K. Ohmi, F. Zimmermann, E. Perevedentsev, Phys. Rev. E 65, 16502, (2002).
- [4] S. Heifets, Wake field of the e-cloud, SLAC-PUB-9025, November 2001.
- [5] S. Heifets, Saturation of the ion induced transverse blowup instability. SLAC-PUB-6959, Jan 1996; International Workshop on Collective Effects and Impedance for B Factories, 12-17 Jun 1995, Tsukuba, Japan. In Tsukuba 1995, Collective effects and impedance for B-factories”, p. 270-287.
- [6] S. Heifets Saturation of the ion transverse instability, SLAC-PUB-7411, January 1997.
- [7] M. Bassetti, G. Erskine, CERN ISR TH/80-06 (1980)
- [8] G.V. Stupakov, T.O. Raubenheimer, and F. Zimmermann, Phys. Rev. E52, 5487 (1995)
- [9] D. V. Pestrikov, Natural BNS damping of the fast ion instability, PRST-Accelerators and beams, V. 2, 044403 (1999)
- [10] G. V. Stupakov, Comment on ”Natural BNS damping of the fast ion instability”, PRST-Accelerators and beams, V. 3, 019401 (2000)
- [11] D.G. Koshkarev and P.R. Zenkevitch, ”Resonance of Coupled Transverse Oscillations in two circular beams”, Part. Accelerators, (1972), V. 3, pp.1-9
- [12] Bellman, R. and Cooke, K.L., Differential-Difference Equations, Academic Press, N.Y. 1963
- [13] M. Pivi, T.O. Raubenheimer, L. Wang, K. Ohmi, R. Wanzenberg, A. Wolski, Simulations of the Electron Cloud Build Up and Instabilities for Various ILC Damping Ring Configurations, SLAC-PUB-12237, March 12, 2007

## 10 Appendix 3. Solution of Eq.(60)

Laplace transform over  $\tau$

$$a(\tau, \zeta) = \int_{-i\infty+c}^{i\infty+c} \frac{d\mu}{2\pi i} \hat{a}(\mu, \zeta) e^{\mu\tau}, \quad (92)$$

reduces Eq. (60) to the Volterra integral equation of the second kind for  $y(z) = \hat{a}(\mu, z)$ ,

$$y(z) + \frac{1}{\mu} \int_0^z dz' K(z - z') y(z') = f(z), \quad (93)$$

where  $f(z) = a(0, z)/\mu$ .

Laplace transform of the kernel gives

$$\hat{K}(p) = \int_0^\infty dz K(z) e^{-pz} = -\frac{\Lambda}{4} \left\langle \frac{\nu^2}{p + (i/2)(1 - \nu^2)} \right\rangle. \quad (94)$$

The solution is given [12] in terms of

$$\hat{R}(p) = \frac{\hat{K}(p)}{\mu + \hat{K}(p)} \quad (95)$$

as

$$\hat{a}(\mu, z) = \frac{a(0, z)}{\mu} - \int_0^z dz' \frac{a(0, z')}{\mu} R(z - z'), \quad R(z) = \int_0^\infty \frac{dp}{2\pi i} \hat{R}(p) e^{pz}. \quad (96)$$

To find  $a(s, z)$ , it is convenient to take the Laplace transform over  $\mu$  first. There are only two singularities at  $\mu = 0$  and  $\mu = -\hat{K}(p)$ . The first pole gives a constant over  $s$  and we drop this term. The second pole gives

$$a(s, z) = \int_0^z dz' a(0, z') \int \frac{dp}{2\pi i} e^{p(z-z') - \hat{K}(p)\tau}. \quad (97)$$

The main contribution in the integral over  $z'$  is given by the upper limit. If  $a(0, z) = a_0$ , then

$$a(s, z) = a_0 \int \frac{dp}{2\pi i} \frac{1}{p} e^{pz - \hat{K}(p)\tau}. \quad (98)$$

The integral over  $p$  in Eq. (97) can be calculated using the saddle-point method. At large  $\tau$ , the saddle points  $|p| \gg 1 - \nu^2$ , and

$$p_\pm = \pm \frac{1}{2} \sqrt{\frac{\Lambda_{eff}\tau}{\zeta - \zeta'}}, \quad \Lambda_{eff} = \Lambda \langle \nu^2 \rangle. \quad (99)$$

One of them,  $p_+$  gives the exponential growth. Then,

$$a(s, z) = \frac{a_0}{\sqrt{2\pi}} \frac{1}{(\Lambda_{eff}\tau\zeta)^{1/4}} e^{\sqrt{\Lambda_{eff}\tau\zeta}}. \quad (100)$$

The result is applicable if  $\Lambda_{eff}\tau/\zeta \gg 1 - \nu^2$ , where

$$\Lambda_{eff} = \Lambda \langle \nu^2 \rangle. \quad (101)$$

Eq. (99) is similar to the result of the linear approximation with  $\Lambda_{eff}$  instead of  $\Lambda$ .

Let us assume the offset  $Y = |A| \cos(\zeta - \tau + \arg A)$  and the Gaussian distribution over the amplitude  $J = A^2$ ,

$$\rho(|A|^2) = \frac{dJ}{J_0} e^{-\frac{J}{J_0}}, \quad (102)$$

where  $J_0/2 = \langle \bar{Y}^2 \rangle = \sigma_c^2$ . Here  $\sigma_c$  is the rms of the cloud at  $\tau$  which we assume to be constant neglecting the pinching effect. Then

$$\begin{aligned} \hat{K}(p) &= \Lambda_{eff}, \\ \Lambda_{eff} &= -\frac{\Lambda}{2} \int_0^\infty \frac{dx \nu^2(J_0 x)}{p + \frac{i}{2}(1 - \nu^2(J_0 x))} e^{-x}. \end{aligned} \quad (103)$$

It is easy to see, that  $\Lambda_{eff}$  decreases for large amplitude  $A$  of particles in the cloud limiting the exponential growth of the linear approximation.